LIQUID STATE DIODES USING POLYMER SEMICONDUCTORS

by

Bedri Gürkan Sönmez

B.S., Electrical and Electronics Engineering, Boğaziçi University, 2009

B.S., Physics, Boğaziçi University, 2009

Submitted to the Institute for Graduate Studies in
Science and Engineering in partial fulfillment of
the requirements for the degree of
Master of Science

Graduate Program in Electrical and Electronics Engineering

Boğaziçi University

2011

ACKNOWLEDGEMENTS

I would like to show my gratitude to some people who made this thesis possible and all hard working hours bearable.

First, I must thank Prof. Şenol Mutlu for endless support and encouragement. When everything seemed to go wrong, he always found a way to overcome problems and kept me tenacious. Without his immense aids, this work could not be completed.

I also would like to thank my lab friends for their sincerity. Modesty and benevolence of Dağhan Gökdel and Baykal Sarıoğlu; supportiveness and comradeship of Engin Afacan, Umut Çindemir, Betül Usta, Mehmet Usta, Orhan Mert, Kürşat Akkurt and Okan Zafer Batur; vast knowledge and brotherhood of Melih Akçakaya and İskender Haydaroğlu will not be forgotten. Especially our conversations about what is best in life with İskender and Melih are priceless.

I am also grateful to my brothers; Adil Enis Arslan, İlker Aslıyüksek, Uğur Durmuş and Vefa Okumuş for sharing their ever-frost hearts with me. They are a reason to wake up for every day.

I owe my deepest gratitude to my parents, Nursel and İsmail Sönmez. Every part of my character carries a sign of them. They will always inspire me in the darkest hours of life.

Finally, I want to thank my beloved wife, Derya. She is my compass in life ocean. Without her, whole life would be nothing but an utter darkness for me.

ABSTRACT

LIQUID STATE DIODES USING POLYMER SEMICONDUCTORS

In this thesis a liquid state polymer diode is fabricated and characterized. First, lateral electrode structures are formed where highly doped p-type Si is used as anode, aluminum is used as cathode and SiO_2 is used as seperation and insulation layer. 40 nm SiO_2 coated Si wafers are purchased and an aluminum layer with thickness of 200 nm is deposited on top of them. By patterning Al layer and dicing the wafer, samples are obtained which carry a $Si/SiO_2/Al$ lateral electrode structure at their sides. After forming electrode structure, polymer solution is prepared. Poly(3-hexylthiophene-2,5-diyl) is used as polymer and dichlorobenzene is used as solvent. Polymer solution is poured onto the $Si/SiO_2/Al$ interface and by applying voltage between electrodes lateral liquid state polymer diode is formed. Fabricated diodes are tested and characterized. Effects of time and solution concentration on performance characteristics are examined. In measurements, 315 mA/cm^2 current density is achieved for 6 mg/ml solution at 7 V which is at least six fold better than the current density of its solid counterpart for the same situation. Also back and forth voltage sweep measurements are applied to investigate hysteresis effect. It is seen that zero current is obtained at -0.7 V when the sweep goes from -10 V to $+10$ V and for reverse sweep zero current is obtained at $+1.4$ V.

ÖZET

SIVI FAZDA POLİMER YARIİLETKEN KULLANAN DİYOTLAR

Bu tezde sıvı fazda polimer diyotlar üretilmiş ve karakterize edilmiştir. İlk olarak; yüksek derecede katkılanmış p-tipi Si anot, Al katot ve SiO_2 ayırıcı ve yalıtıcı katman olacak şekilde yüzeyel elektrot yapıları oluşturulmuştur. 40 nm SiO_2 ile kaplı Si pullar satın alınmış ve üzerleri 200 nm alüminyum tabakası ile kaplanmıştır. Al tabakasının şekillendirilmesi ve pulun kesilmesi ile yan yüzeylerinde $Si/SiO_2/Al$ yüzeyel elektrot yapısı taşıyan örnekler elde edilmiştir. Elektrot yapısı oluşturulduktan sonra, polimer çözeltisi hazırlanmıştır. Polimer olarak poly(3-hexylthiophene-2,5-diyl), çözücü olarak ise diklorobenzen kullanılmıştır. Polimer çözeltisi $Si/SiO_2/Al$ arayüzüne dökülmüş ve elektrotlar arasına potansiyel fark uygulanarak yüzeyel sıvı fazda polimer diyot oluşturulmuştur. Üretilen diyotların sınaması ve karakterizasyonu gerçekleştirilmiştir. Zaman ve çözelti yoğunluğunun performans özelliklerine etkileri incelenmiştir. Ölçümlerde 6 mg/ml çözeltide, 7 V için 315 mA/cm^2 akım yoğunluğuna ulaşılmıştır ki bu değer aynı durumdaki katı eşdeğer diyottakinden en az altı kat daha yüksektir. Ayrıca ardıl izlem etkisini incelemek amacıyla ileri ve geri potansiyel fark süpürümü uygulanmıştır. Süpürüm -10 V değerinden $+10$ V değerine doğru uygulandığında sıfır akım -0.7 V değerinde, süpürüm ters yönde uygulandığında ise sıfır akım $+1.4$ V değerinde elde edilmiştir.

TABLE OF CONTENTS

LIST OF FIGURES

LIST OF SYMBOLS

A^*	Richardson's constant
Al	Aluminum
d	Polymer thickness
D	Diffusion coefficient
DCB	Dichlorobenzene
E_g	Bandgap energy
E_t	Trap energy
F	Electric field
F_{sat}	Electric field at saturation voltage
g	Degenerecy
h	Planck's constant
HF	Hydrofluoric acid
J	Current density
k_B	Boltzmann's constant
m^*	Effective charge carrier mass
M_n	Polymer number-averaged molecular weight
n	Spatially varying electron concentration
n_0	Intrinsic electron concentration
n_{inj}	Injected free electron concentration
N_s	Number of availible states per unit volume
n_t	Trapped electron concentration
N_t	Total trap density
q	Elementary charge
SiO_2	Silicon dioxide
T	Temperature
$\mathcal{V}$	Effective voltage across the polymer layer
V_J	Injection-dominating voltage
V_{TFL}	Trap-filling voltage

ε_0	Vacuum permittivity
ε_r	Relative dielectric constant
μ	Charge carrier mobility
ϕ_0	Zero-field injection barrier
Φ_A	Anode work function
Φ_{BI}	Built-in potential
Φ_C	Cathode work function
Φ_e	Electron injection barrier
Φ_h	Hole injection barrier

LIST OF ACRONYMS/ABBREVIATIONS

CZ	Czochralski
FN	Fowler-Nordheim
HOMO	Highest Occupied Molecular Orbital
HT	Head-to-Tail
I-V	Current-Voltage
IPA	Isopropyl Alcohol
LED	Light-Emitting Diode
LUMO	Lowest Unoccupied Molecular Orbital
OLED	Organic Light-Emitting Diode
P3HT	poly(3-hexylthiophene)
PLED	Polymer Light-Emitting Diode
PTFT	Polymer Thin Film Transistor
PR	Photoresist
RFID	Radio-Frequency Identification
RS	Richardson-Schottky
SCLC	Space-Charge Limited Current
SEM	Scanning Electron Microscopy
TCLC	Trap-Charge Limited Current
UV	Ultraviolet

1. INTRODUCTION

Since the discovery of polymer semiconductor [1], which was awarded with Nobel Prize in Chemistry, polymer electronics have made a remarkable process. In spite of the fact that their performances are still inferior to their inorganic counterparts, there are fields in which poor performance is tolerable in return of some advantages that polymer electronics can provide.

It would be wrong to consider polymer electronics as a replacement for contemporary silicon technologies. It is more like an alternative solution where single crystalline silicon technologies are highly inefficient or practically impossible. Greatest benefit of the polymer electronics lies behind its low-cost nature. Cheap process methods such as spin-coating, drop-casting or inkjet-printing make polymer electronics a perfect solution for applications which are disposable because using expensive materials for single use applications can make them cost-prohibitive [2–4].

Electrochemical sensors and biosensors are good application areas for polymer electronics. Electrical conductivity of polymers can change drastically due to environmental factors which makes them convenient for sensory applications. Some conductive polymers are biocompatible and they can be used in biosensors [5, 6].

Radio-frequency identification (RFID) tag is another application field for polymer electronics. RFID tags are wireless smart circuitries which are used for pricing or anti-theft purposes. They have antennas and logic circuitries which can take the outside transceiver's signal and transmit some data back. RFID tags are placed on goods, therefore they should be lightweight and inexpensive. Furthermore, very high speed operation is not necessary for those circuitries. Such systems can be manufactured with polymer electronics [7].

Large area illumination and flexible flat panel displays are the largest commercial applications of polymer electronics. Due to semiconductor nature of conjugated poly-

mers, diodes and transistors can be made from them. With proper process schemes and polymer choice, these diodes can emit light at desired wavelengths. Such devices are called organic light-emitting diodes (OLED) or more specifically polymer light-emitting diodes (PLED). Inorganic LEDs are limited with die sizes and cost-inefficient for large area display systems. However, with cheap process and patterning techniques of polymer electronics, such large area production is feasible. For flexible flat panel displays, polymer thin film transistors (PTFT) are used. Large area PTFTs can be produced with inkjet printing technique. This method is applicable on flexible surfaces such as plastic or even paper which enables roll-to-roll production. Therefore, it provides a huge advantage to polymer systems over the inorganic counterparts which are produced on brittle and rigid substrates [8,9]. Also solar cells are one of the application fields of polymer electronics. Solar cells produce electricity from sunlight. Although polymer-based solar cells cannot reach the efficiency of inorganic-based ones; cheap, robust production techniques and easy implementation to large areas make them an option [10].

Scientists and engineers are still working on polymer semiconductors to be able to extend application fields. New areas emerge with advances in polymer technologies. Improvements in production costs, product lifetimes and device performances can pave the way for new applications which are not even considered today due to technological limitations. Therefore, it is a hot research topic to optimize existing process techniques and come up with new methods to overcome several weaknesses which is the motivation of this thesis.

Outline of the thesis is as follows: In Chapter 2, an overview of polymer electronics is made. Detailed information about theoretical background and device physics is given. In Chapter 3, liquid state diodes are introduced. Working principles, production stages and characterization of fabricated devices are demonstrated. In Chapter 4, a conclusion is made and possible future work is discussed.

2. OVERVIEW OF POLYMER ELECTRONICS

2.1. Bonding and Conduction Mechanism

Polymers are large molecule chains which have repeating structural units. These units are composed of carbon, hydrogene and some other atoms. Carbon atoms are connected to each other by alternating single and multiple bonds. Such a system is called as conjugated system and it forms the backbone of a conjugated polymer.

To understand the conduction mechanism in a conjugated polymer, one has to focus on the atomic structure of the carbon atom. Carbon has $1s^2 2s^2 2p^2$ electronic configuration. Therefore, it has 4 electron in the outer-shell. When two carbon atoms come close, wavefunctions of these outer-shell electrons tend to overlap and form hybridized orbitals which allows better coupling with the other atom [11]. An illustration of these hybrid orbitals can be seen in Figure 2.1.

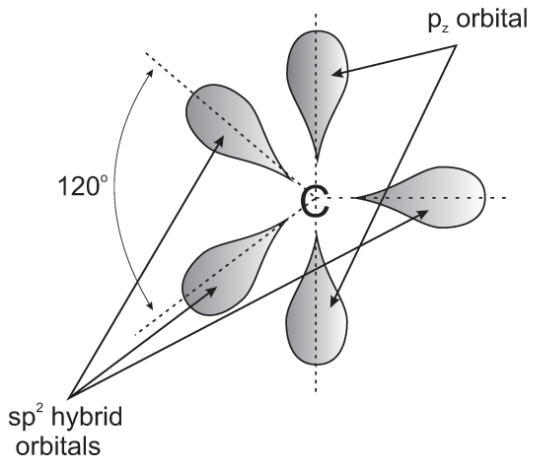

Figure 2.1. sp^2 and p_z orbitals in carbon atom.

Three hybrid sp^2 orbitals stay in a plane and make 120° angle with each other. p_z orbital, however, stays orthogonal to this plane. When carbon atoms come together, sp^2 orbitals of neighbor atoms overlap and produce a strong bond which is called as σ-bond. This phenomenon is depicted in Figure 2.2. This bond is so strong that electrons

which form this bond are highly localized and cannot contribute to conduction process. The conduction system is formed by p_z orbitals. In the bonding process, p_z orbitals also overlap and constitute π orbitals. Electrons in these π orbitals are highly delocalized and can move from one atom to another easily. Therefore, charge carrier conduction can be sustained via these conjugated π orbitals throughout the polymer chain.

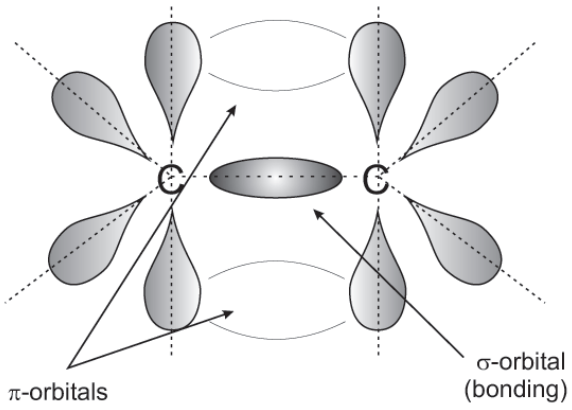

Figure 2.2. σ-bond and π orbitals in carbon atoms.

In the formation of π orbitals, wavefunctions of p_z orbitals play a crucial role. Electronic wavefunction of a p orbital has a phase component. So, two overlapping p_z orbitals either have parallel phases or anti-parallel phases. If they have parallel phases, that results in constructive interference of wavefunctions and π bonding orbitals are constructed. However, if their phases are anti-parallel, wavefunctions interfere destructively and π^* anti-bonding orbitals are constructed [12, 13]. This process is shown in Figure 2.3.

If we consider the whole polymer chain, these π bonding and π^* anti-bonding orbitals form π and π^* energy bands. The former is called as the highest occupied molecular orbital (HOMO) and the latter is called as the lowest unoccupied molecular orbital (LUMO). These energy bands can be seen as the counterparts of valence and conduction bands of inorganic semiconductors, respectively [14, 15].

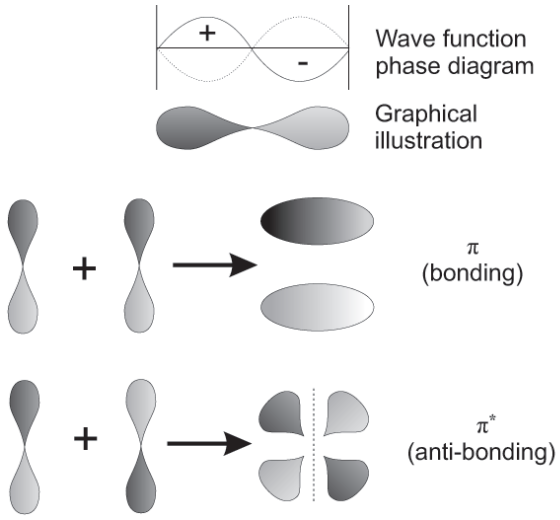

Figure 2.3. Formation of π bonding and π^* anti-bonding orbitals.

2.2. Energy Bands

General usage of polymers in electronic applications is as solid thin films. Therefore, lots of polymer chains stay together as a spaghetti-like pile. A charge carrier can move throughout a chain's π orbital or can jump to adjacent chain's π orbital. Such a jump between two localized sites is called as hopping and that is the dominating inter-chain charge carrier transfer in polymers. In spite of the fact that it is much slower than the intra-chain charge carrier transfer, it provides long range conduction in bulk quantities. However, charge carrier mobilities are too low with respect to inorganic semiconductors due to this hopping mechanism [16, 17].

Dealing with lots of polymer chains together requires unifying models. So, it is convenient to use band diagrams which is used for inorganic semiconductors. Although disordered nature of bulk polymers and inherent traps prevent them having well-defined band structures [18], it is still a good approximation for gaining insight. Concepts like bandgap, potential barriers, conduction and valence bands (as LUMO and HOMO) can be defined for polymer semiconductors. In Figure 2.4, electronic band structure of a polymer semiconductor between two electrodes can be seen. Here, Φ_A is anode work function, Φ_C is cathode work function, Φ_h is hole injection barrier, Φ_e is

electron injection barrier, Φ_{BI} is built-in potential, V is applied voltage, $\mathcal{V}$ is effective voltage across the polymer layer and q is elementary charge. Energy levels and current injection under forward bias are depicted as they are in an inorganic semiconductor.

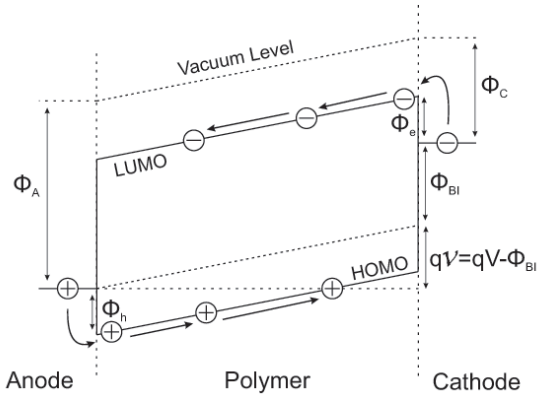

Figure 2.4. Band diagram of a polymer semiconductor which is sandwitched between two electrodes under applied bias. After [18].

Band gap is an important metric for polymer semiconductors as it is for inorganic ones. We can approximately calculate a polymer's band gap as the separation of HOMO and LUMO. Polymers generally have wide band gaps which are typically in the 1.5-3.5 eV range for the ones used in devices [19]. From band gap energy, we can calculate the intrinsic carrier concentration by the formula [20] which is derived for inorganic semiconductors as

$$n_0 = N_s \exp\left(-\frac{E_g}{2k_B T}\right) \tag{2.1}$$

where n_0 is intrinsic carrier concentration, N_s is the number of availible states per unit volume, E_g is band gap energy, k_B is Boltzmann's constant and T is the absolute temperature in Kelvin. N_s is a material-dependent value which changes with temperature. If we take N_s as of order $\sim 10^{19}$ cm^{-3} for room temperature [20] and calculate n_0 values for polymers with aforementioned band gap energies, we can see that these values are very low ($\ll 10^{10}$ cm^{-3}). This means that polymer semiconductors have negligible thermally generated free carriers and they are like insulators in this point of view.

2.3. Charge Carrier Injection

Two basic mechanism can be used for charge carrier injection from a contact to a semiconductor: Richardson-Schottky (RS) thermionic emission and Fowler-Nordheim (FN) tunnelling [21]. RS thermionic emission depends on lowering the image-potential by application of an external electric field. In metals, free electrons are bound to bulk of the material. Therefore, when an electron tries to leave the conductor, it experiences a force due to an image-charge which pulls it back. To be able to release an electron from the electrode, one has to overcome the force due to image-charge. In RS thermionic emission, it is done by an applied external field $F = \mathcal{V}/d$ where $\mathcal{V}$ is the effective voltage across the polymer and d is the thickness of polymer layer. Current density in RS thermionic emission is calculated as

$$J_{RS} = A^* T^2 \exp\left(-\frac{\phi_0 - \sqrt{\frac{q^3 F}{4\pi\varepsilon_0\varepsilon_r}}}{k_B T}\right) \tag{2.2}$$

where A^* is Richardson's constant, ϕ_0 is zero-field injection barrier, q is elementary charge, ε_0 is vacuum permittivity and ε_r is relative dielectric constant of polymer.

In FN tunnelling, electrostatic effects are neglected and electrons are assumed to tunnel through the triangular potential barrier from electrode to polymer. This time, current density is calculated as

$$J_{FN} = \frac{A^* q^2 h^2 F^2}{32\phi_0 k_B \pi^2 m^*} \exp\left(-\frac{8\pi\sqrt{2m^*{\phi_0}^3}}{3qhF}\right) \tag{2.3}$$

where h is Planck's constant and m^* is effective electron mass.

RS thermionic emission and FN tunnelling are both valid for charge injection from electrode to semiconductor under proper situations. However, they both assume that the semiconductor has well defined band structure and long rage order. This assumption cannot hold for polymer semiconductors due to the disordered nature of these materials. Polymeric solids have traps at various energy levels and short

average mean free path for charge carriers. Such obstacles impede to injection process and cause some of the injected carriers being reflected back into the electrode which complicates the mechanism [18].

2.4. Conduction Regimes

Once charge carrier injection is achieved, conduction inside is dominated by various mechanism for different operation conditions. Physics of these mechanisms are too complicated and related differential equations can only be solved numerically. However, analytical solutions are possible only for some special cases. Therefore, various assumptions are made to derive basic relations. In calculations, it is assumed that charge carrier transport includes one type of charge carrier (only electrons or only holes) which is actually the general case for polymer semiconductors. A specific polymer generally can conduct one charge carrier type well which defines its type. For example a p-type polymeric semiconductor has relatively good hole mobility and poor electron mobility. This characterization differs from inorganic semiconductors. A p-type semiconductor has abundant of positive charge carriers, therefore conduction is obtained generally by holes. However, polymers have very little amount of intrinsic carriers, therefore type shows which injected carrier is being transferred easily relative to other one. Another assumption is that charge carrier mobility μ and dielectric permittivity ε are constant throughout the material and independent of the external field.

2.4.1. Ohmic Regime

It is convenient to start with basic equations for semiconductors to gain insight about the conduction mechanisms. Transport equation which includes drift and diffusion currents can be written as

$$J = qn\mu F - qD\frac{\mathrm{d}n}{\mathrm{d}x} \tag{2.4}$$

where n is spatially varying free electron concentration and D is diffusion coefficient. Electron is chosen as the charge carrier type but derivations are the same for holes, so obtained equations hold for both charge carrier types. In the steady-state condition, diffusion dominates only at very near of the electrode and drift dominates for the rest of polymer layer. Therefore, one can neglect the diffusion term in Equation 2.4 and new transport equation becomes

$$J = qn\mu F. \tag{2.5}$$

We can take $n = n_0 + n_{inj}$ where n_0 is intrinsic free electron concentration and n_{inj} is injected free electron concentration. Normally n_0 is a very small number and can be neglected. However, for situations in which external field is very low, charge carrier injection level can be lower than number of intrinsic carriers. This operation region is called ohmic region and if we replace $F = \mathcal{V}/d$ in Equation 2.5, it becomes

$$J_{ohm} = qn_0\mu\frac{\mathcal{V}}{d} \tag{2.6}$$

where J_{ohm} is the current density in the ohmic region. Equation 2.6 shows why this region is called as ohmic. Current density is linearly proportional to the effective voltage across the polymer.

2.4.2. Space-Charge Limited Current (SCLC) Regime

For higher external fields, $n_{inj} \gg n_0$ so we can neglect n_0 and take $n \approx n_{inj}$ which means that polymer semiconductor is assumed to be a perfect insulator which has no intrinsic charge carriers. If we also assume that it has no traps, then we can write the Poisson equation as

$$\frac{\varepsilon_r\varepsilon_0}{q}\frac{\mathrm{d}F}{\mathrm{d}x} = n \tag{2.7}$$

and by replacing it in Equation 2.5 we obtain

$$J = \varepsilon_r \varepsilon_0 \mu F \frac{\mathrm{d}F}{\mathrm{d}x}. \tag{2.8}$$

Now, we should arrange Equation 2.8 as

$$J\,\mathrm{d}x = \varepsilon_r \varepsilon_0 \mu F\,\mathrm{d}F \tag{2.9}$$

and take the integral of both sides

$$J \int_0^x \mathrm{d}\tau = \varepsilon_r \varepsilon_0 \mu \int_0^F \xi\,\mathrm{d}\xi \tag{2.10}$$

which gives us

$$\sqrt{\frac{2J}{\varepsilon_r \varepsilon_0 \mu}} x^{\frac{1}{2}} = F. \tag{2.11}$$

If we take the integral of both sides one more time, we obtain

$$\sqrt{\frac{2J}{\varepsilon_r \varepsilon_0 \mu}} \int_0^d x^{\frac{1}{2}}\,\mathrm{d}x = \int_0^d F(x)\,\mathrm{d}x \tag{2.12}$$

and by assuming that electric field is zero at the electrode which gives the boundary condition $F(0) = 0$, then right hand side of the integral becomes the effective voltage, $\mathcal{V}$. Therefore, we obtain

$$\frac{2}{3}\sqrt{\frac{2J}{\varepsilon_r \varepsilon_0 \mu}} d^{\frac{3}{2}} = \mathcal{V} \tag{2.13}$$

which, by leaving J alone, turns to Mott-Gurney equation [22]

$$J_{SCLC} = \frac{9}{8} \varepsilon_r \varepsilon_0 \mu \frac{\mathcal{V}^2}{d^3}. \tag{2.14}$$

In Equation 2.14, J_{SCLC} stands for the current density in space-charge limited current (SCLC) region. In this region, $n_{inj} \gg n_0$ so injected charge carriers constitute space charges in polymer layer which limits the current.

2.4.3. Velocity Saturated SCLC Regime

An extreme case occurs in SCLC region where velocity saturation is reached. After that point, charge carrier velocity approaches an upper limit and does not change with increasing field. To calculate the current density after that point, F should be replaced by F_{sat} in Equation 2.9 as

$$J\,\mathrm{d}x = \varepsilon_r \varepsilon_0 \mu F_{sat}\,\mathrm{d}F. \tag{2.15}$$

Again we should take the integral of both sides

$$J\int_0^x \mathrm{d}\tau = \varepsilon_r \varepsilon_0 \mu F_{sat}\int_0^F \mathrm{d}\xi \tag{2.16}$$

which gives us

$$\frac{Jx}{\varepsilon_r \varepsilon_0 \mu F_{sat}} = F. \tag{2.17}$$

If we take the integral of both sides one more time, we obtain

$$\frac{J}{\varepsilon_r \varepsilon_0 \mu F_{sat}}\int_0^d x\,\mathrm{d}x = \int_0^d F(x)\,\mathrm{d}x. \tag{2.18}$$

With the same assumptions in the SCLC derivation, after leaving J alone and replacing $\upsilon_{sat} = \mu F_{sat}$ we obtain

$$J_{SCLC,sat} = \frac{2\varepsilon_r \varepsilon_0 \upsilon_{sat} \mathcal{V}}{d^2} \tag{2.19}$$

where v_{sat} is the charge carrier velocity in saturation region. From Equation 2.19 it can be seen that current density is again linearly proportional to effective voltage across the polymer.

2.4.4. Trap-Charge Limited Current (TCLC) Regime

Up to now, it is assumed that polymer semiconductor has no traps, however it is quite unlikely especially for polymeric solids. Entangled and disordered nature of polymer chains when they are in bulk form causes ocurrance of trap states. Trap states do not contribute to conduction, but they increase space charges by trapping charge carriers, therefore they cause alteration in the current density. If trap energy is on the order of k_BT it is called as a shallow trap, if it is much larger than k_BT then it is called as a deep trap [15]. For shallow traps, thermal de-trapping is also possible, therefore it only causes a slight variation in the current density. However, deep traps are more problematic and strongly affects the conduction behavior [23].

If we assume that traps stay in discrete levels, we can calculate trapped electron concentration n_t as [18]

$$n_t = N_t \left[1 + g^{-1} \exp\left(\frac{E_t - E_F}{k_B T}\right)\right]^{-1} \tag{2.20}$$

where N_t is total trap density, E_t is trap energy, E_F is Fermi level and g is degeneracy. By using n_t, we have to arrange Equation 2.14 as [23]

$$J_{TCLC} = \frac{9}{8}\left(\frac{n}{n + n_t}\right)\varepsilon_r \varepsilon_0 \mu \frac{\mathcal{V}^2}{d^3} \tag{2.21}$$

where J_{TCLC} stands for trap-charge limited current density. After a specific voltage value V_{TFL}, traps are filled and current density behavior turns to SCLC regime again. This critical voltage value is calculated as [24]

$$V_{TFL} = \frac{qN_t d^2}{\varepsilon_r \varepsilon_0}. \tag{2.22}$$

If trap states do not stay at discrete levels but are distributed in energy levels, calculation becomes complicated. In the case of an exponential distribution which is generally used for organic materials, n_t takes the form of

$$n_t = \int_{-\infty}^{E_C} \frac{\frac{N_t}{E_t} \exp\left(\frac{E-E_C}{E_t}\right)}{1 + g^{-1} \exp\left(\frac{E-E_F}{k_B T}\right)} \mathrm{d}E \tag{2.23}$$

and by using this n_t value current density can be derived as [18, 25, 26]

$$J_{TCLC} = N_C \mu q \left(\frac{\varepsilon_r \varepsilon_0 \alpha}{N_t q(\alpha+1)}\right)^{\alpha} \left(\frac{2\alpha+1}{\alpha+1}\right)^{\alpha+1} \frac{\mathcal{V}^{\alpha+1}}{d^{2\alpha+1}} \tag{2.24}$$

where $\alpha = E_t/k_B T$. Due to the fact that $(\alpha+1) > 2$, current density is proportional to a higher exponent of effective voltage than its square in this situation.

2.4.5. Overall Look

In Figure 2.5 all regimes are illustrated for a polymer which have discrete trap levels and current depends on one type of charge carrier.

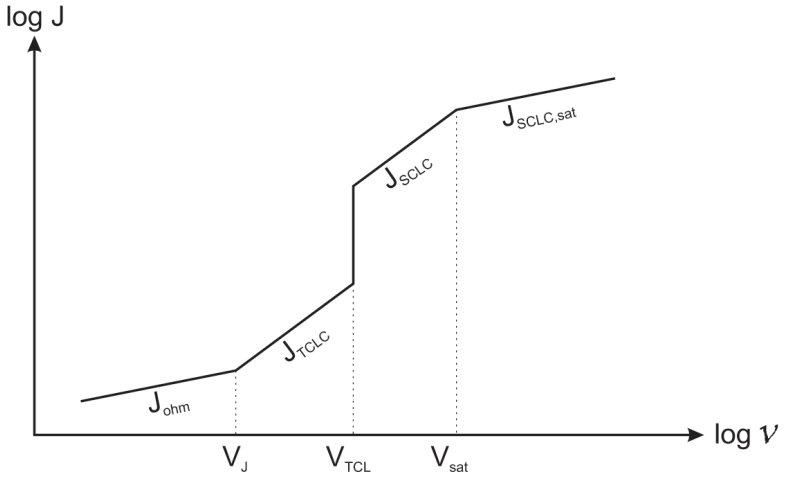

Figure 2.5. Conduction regimes in logarithmic scale.

For very low voltage values, conduction is in the ohmic regime and current density is linearly proportional to $\mathcal{V}$. After a point, $\mathcal{V} = V_J$, injected charge carriers start to

dominate and conduction goes into SCLC regime. However, there are trap states in the polymer and current is altered by trap charges. Here, current density is proportional to $\mathcal{V}^2$ but current level is lower than what is expected for SCLC. Therefore, this region is called TCLC regime. After the critical voltage, $\mathcal{V} = V_{TCL}$, trap states are filled and current density level shows a sharp elevation. Conduction enters the trap-free SCLC regime and current density is proportional to $\mathcal{V}^2$ with a higher level than TCLC. If applied voltage is kept increasing, system goes into velocity saturation and after the point, $\mathcal{V} = V_{sat}$, conduction is in the velocity saturated SCLC regime. Current density is linearly proportional to $\mathcal{V}$ again and it holds this relationship for further increasing voltage values [27].

3. LIQUID STATE DIODES

3.1. Motivation

Operation mechanisms of polymer semiconductors are described in Chapter 2. Several points, which directly influence operation characteristics, should be emphasized. As mentioned before, conduction mechanism in polymer semiconductor depends on π orbitals. Overlapping in π orbitals determines the intra-chain conduction quality. The chain geometry plays an important role in this overlapping mechanism. In bonding process of two neighbour atoms, sp^2 hybrid orbitals stay in a plane for each of them. If two atom share the same plane, it causes well overlapping between p_z orbitals. However, if there is an angle between two planes, which means polymer chain shows a helical orientation, then overlapping between p_z orbitals decreases which leads to a deterioration in conduction performance.

Another important point is the long rage order. In polymers, charge carriers are transferred via π orbitals in intra-chain conduction process. However, inter-chain conduction depends on hopping in which mobility is drastically low relative to $\pi-\pi$ conduction process. In the absence of long range order, charge carriers are forced to hopping between localized energy sites and conduction process becomes more hopping dependent as long as disorder increases [28]. This amorphous structure is the general feature of polymeric solids. For device applications, polymer semiconductors are used as solid thin films. Such films are prepared by several techniques such as spin-coating, dip-coating or drop-casting. In these methods, polymer solution is prepared with a proper solvent material and this solution is applied to the surface where we need the polymer thin film. Afterwards, solvent in the solution is evaporated and thin film is formed. For some polymers, which have low molecular weight, direct deposition by thermal evaporation of polymer itself is an option. Yet, for both processes obtained solid thin films show disordered orientation which causes amorphous structure. Polymer chains tend to accumulate in a spaghetti-like fashion and long rage order cannot be attained.

Degradation is also an issue for polymer structures. Devices which depend on polymer electronics have limited lifetimes. Either environmental effects or inward chemical reactions cause degradation in the polymer material and alter the operation efficiency. Due to the fact that degradation process for polymeric structures are generally faster than inorganic ones, endurance of the polymer part determines the operational lifetime of device. Immobile nature of solid films makes them irreplaceable in deterioration situations and causes whole device being useless.

Here a new approach, liquid state diode, is presented which is a candidate of possible solution for problems mentioned above. This approach depends on using the polymer semiconductor not in solid phase but in liquid phase as a solution. It is known that some polymers tend to stay separate from each other instead of entangling in liquid state [29]. It also decreases the possibility of self-entangling of polymer chain and provides a more linear geometry which is very important for π orbitals. Again by selecting proper polymer-solvent combination, planar arrangement of molecules where all sp^2 hybrid orbitals share the same plane can be achieved. By such orientation intra-chain charge carrier mobilities can be maximized [30].

In the absence of self-entanglement, polymer chains tend to be present as separate flexible rod-like structures in solution. For proper chain lengths, these structures can be treated as nano-rods. This morphology provides good intra-chain charge carrier mobilities, however the separation between polymer chains in solution makes hopping process harder, therefore inter-chain conduction decreases drastically. Because of this fact, to be able to obtain efficient charge carrier conduction, one should assure that all conduction should be carried on by intra-chain transfer. For this purpose, distance between electrodes should be smaller than chain length to overcome the necessity of inter-chain hopping.

Another advantage of using polymer semiconductor in liquid state is possible renewability. Although solid thin films are compact and stationary, solution-based polymers are ambulatory and fluidic. Therefore, with proper transfer system, polymer solution can be relocated easily. If there are devoted microchannel systems, solution-

based polymer part can be refreshed when degradations occur. Moreover, such a system can provide possibility of using different kind of polymer solutions with the same system. Again with a proper channel network, one polymer solution can be replaced by another. Due to the fact that every different polymer has its own characteristics and functions, multi-functional devices can be designed via this kind of approach.

With aforementioned advantages, liquid state polymer semiconductors can propose solutions to some problems which their solid counterpars have. They also are capable of producing their own applications which may not be feasable with solid polymer layers. In this work diodes, which use liquid state polymer semiconductors, are fabricated and characterized. A diode structure is preferred because it is the basis for whole electronic structures and a convenient testing device for searching effects of variable factors.

3.2. Fabrication Process

3.2.1. Polymer Selection

First element of a liquid state diode is a soluble polymer semiconductor. In this work, poly(3-hexylthiophene-2,5-diyl)(P3HT) is used. P3HT is a member of the polythiophene family [29] on which a considerable amount of research has been done [31–34]. P3HT is a p-type conjugated polymer semiconductor, therefore the main charge carriers are holes. It has the highest hole mobility between the solution-processable polymers which can be up to 0.1 cm^2/Vs for regioregular ones [35, 36]. Regioregular means that sp^2 hybrid orbitals are aligned as coplanar which leads to a highly conjugated polymer chain. Such order also provides a relatively field independent and weakly temperature dependent charge carrier transfer [37] which makes P3HT highly desirable.

The P3HT, which is used in this work, is synthesised and purified by Sigma-Aldrich Co. Its linear formula is $(C_{10}H_{14}S)_n$ and polymer number-averaged molecular weight, M_n, is approximately 8.7×10^4. It has a head-to-tail (HT) type of regioregu-

larity. According to the manufacturer's notes, regioregularity percentage of the P3HT is estimated as 98%. In Figure 3.1 a P3HT chain can be seen.

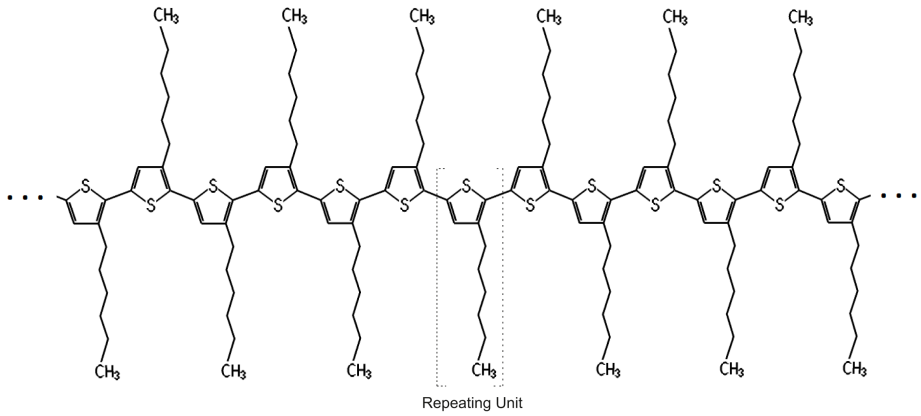

Figure 3.1. A P3HT chain. One repeating unit is indicated by dashed lines.

Such a straight and well-oriented P3HT chain behaves like a nano-rod which has a molecular thickness of around 0.4 nm orthogonal to benzene rings and around 1.7 nm in the direction of side chains with a variable longitudional length which depends on the molecular weight [38]. From calculations depending on M_n it is estimated that an average chain includes approximately 520 repeating units. By taking one repeating unit length as 0.39 nm [29], average chain length is estimated as 200 nm which is an important metric for electrode separation.

Another concept which should be mentioned here is persistence length. It basically shows the stiffness of the polymer chain [39]. For shorter polymer pieces than persistence length, polymer behaves as a stiff rod. However, if the piece length is much greater than the persistence length, then polymer should be considered as a three-dimensional object. Therefore, it is important for the geometry of polymer chain in solution. The persistence length for P3HT is 2.4 ± 0.3 nm which means that chains with 200 nm length can be considered as nonaggregerated flexible coils in solution [29], however the value should be kept in mind.

P3HT is soluable in chloroform, trichlorobenzene, dichlorobenzene, toluene and xylenes. We used dichlorobenzene (DCB) to prepare P3HT:DCB solutions with various

concentrations.

3.2.2. Electrode Fabrication

In electrode fabrication process, there are three important aspects: electrode seperation, electrode materials and diode structure. As mentioned in Section 3.1 electrode seperation must be comparable to chain length which means that distance between two electrodes can be 200 nm at most. However, it is for the best case in which polymer chains are alligned perpendicular to electrodes and stay as perfectly stiff nano-rods. Any kind of chain-electrode alignment except orthogonal requires a narrower electrode seperation to ensure that both ends of the chain are in contact with electrodes. Small deviations from stiff nano-rod approximation due to persistence length can also affect the seperation distance.

In combination with the electrode seperation, diode structure is also important. A proper way with a polymer solution would be a point-contact diode structure. An example for such structure can be seen in Figure 3.2. Point-contact diode structure has an easy fabrication process and provides a huge flexibility about the variables. It is suitable for trying different solutions and manipulating the distance between electrodes.

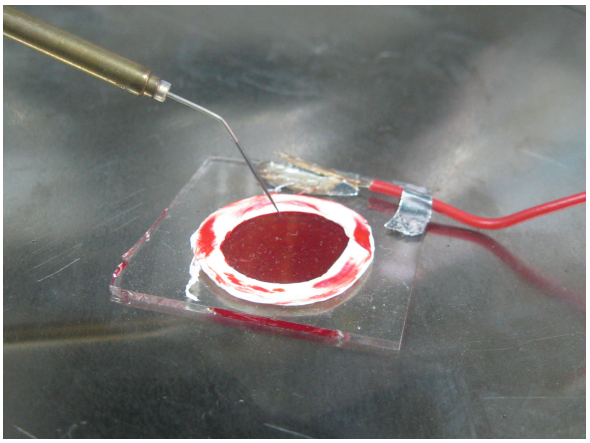

Figure 3.2. An example for a point-contact diode. Solution is dripped onto the planar electrode and the needle-like electrode is merged into the solution.

Yet, it also has some drawbacks. For our purpose, distance between electrodes should be smaller than 200 nm and it is nearly in the error margin of distance arrangement mechanism for such system. A more stable and delicate spacing arrangement is needed. Another problem is the cross-sectional area of needle-like diode. It introduces a high asymmetry between electrodes which affects the orientation of electric field lines and it is not preferred. Drying of solution is also a problem which prevents taking measurement for long time spans.

A vertical diode structure could be a solution for fine distance arrangement problem. In Figure 3.3 a schematic for such structure is presented. Two parts can be patterned and assembled to form the vertical diode. On bottom part, spacers can be deposited and patterned so steady spacing can be achieved between two electrodes. After polymer solution is dripped onto the bottom part, top part can be placed and a sandwich system is formed. This structure also slows the drying process due to decreased environmental interaction of polymer solution.

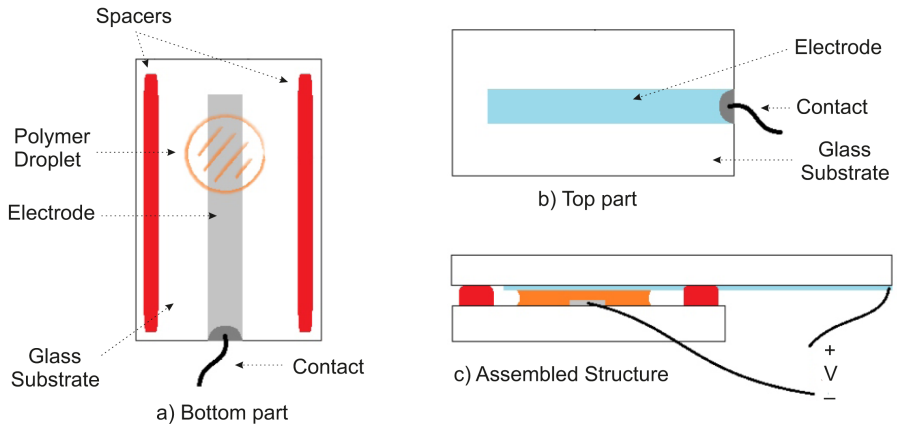

Figure 3.3. Illustration of a vertical diode which uses polymer solution as active area.

The problem about the vertical diode structure is the complicated fabrication and limited flexibility of the setup. Every diode structure should be prepared with intensive care because once the system is assembled, no manipulation can be done on it. If a defect occurs during the measurement, system becomes useless and a new one should be fabricated with all parts. Moreover, distance control is not good enough

for our purposes. Although intact spaces provides a better stability, it is not easy to produce them under the thickness of 200 nm. Even in that case, substrate of the top part can bend and result in short circuit of electrodes. This bending cannot be neglected in nanometer range and spoils the distance control.

We decided to use a lateral diode structure after examining other options. In lateral diodes, electrode structure is formed on a substrate and polymer solution is poured on this pattern. The difficulty about this scheme is obtaining two electrodes with small proximity from different materials. When two electodes are made from the same material, diode efficiency decreases drastically due to unmatched energy levels. To overcome this problem, we produced lateral diode structures not on the surface but at the cross-section.

Idea depends on the fact that it is not easy to produce different materials very near to each other on the surface, however they can easily be deposited on top of each other. So, a dielectric layer can be deposited on the first electrode material. Then, second electrode layer is deposited and patterned on this dielectric material. Dielectric layer provides electrical insulation between two electrodes and by adjusting its thickness, desired seperation values can be reached. Once insulation layer is deposited, it becomes an intact spacer which provides a good and stable seperation distance control. After the deposition of top electrode layer is finished, electrode structures can be patterned and whole layer can be diced to obtain small samples which carries the desired electrode structure at their sides.

In Figure 3.4 designed lateral diode structure can be seen. Diode structure is obtained at one side which has the interface of two electrodes and seperation layer. Second electrode is patterned in this way to be able to prevent any unwanted contacts between electrode layers due to possible contamination of other sides. Polymer solution is dripped to this interface side and lateral diode is realized. It has the stability of vertical diode strucute and fabrication ease of point-contact diode structure. Moreover, it provides delicate control on electrode seperation. The only drawback about this structure is being prone to solution drying.

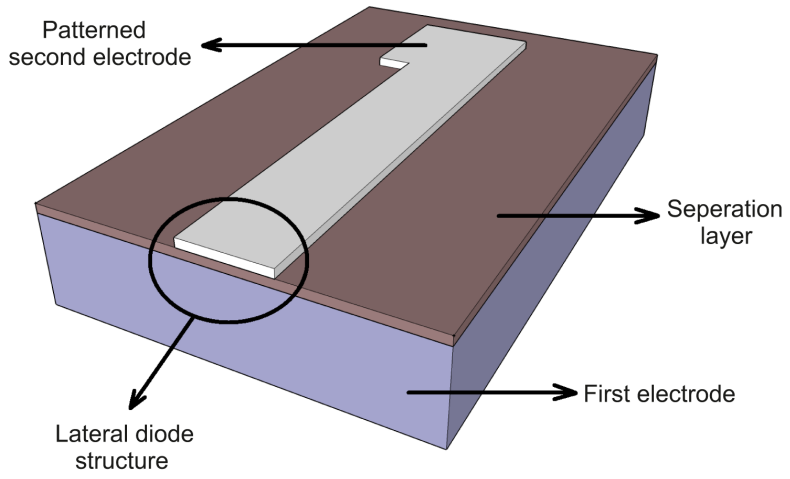

Figure 3.4. Illustration of lateral diode structure.

Electrode materials are critical for device efficiency. Differences between electrode work functions and polymer energy levels should be as small as possible for efficient charge carrier injection. Regioregular P3HT has -5.2 eV HOMO and -3.0 eV LUMO levels [40]. A highly doped p-type silicon can be used as first electrode. Its work function is -4.9 eV [41] which makes it a good candidate for anode and it also has a natural oxide which can be used as the insulating seperation layer. For cathode, aluminum can be used with work function of -4.3 eV. It is not matched well with the LUMO level of P3HT, however environmental stability and easy deposition of Al makes it suitable for our diode structure. If silicon is used as anode, separation layer turns out to be SiO_2. Its thickness decides the electrode seperation, therefore it is an important metric. It should be thinner than 200 nm as mentioned before. However if it becomes too thin, problems about tunnelling and dielectric breakdown emerge. SiO_2 has dielectric strength around 10^7 V/cm [21]. We decided the thickness of oxide layer as 40 nm. It is a good value for stiff rod-like chain approximation and it can stand potential differences up to 40 V in theory.

$4''$ p-type silicon wafers are purchased from Silicon Quest International, Inc. Wafers are Boron doped CZ silicon which have thickness of 500 μm and resistivity of $0.01 - 0.02$ Ωcm. They also have thermally grown oxide with mean thickness of

418.4 Å. On top of SiO_2, Al layer is deposited by sputtering.

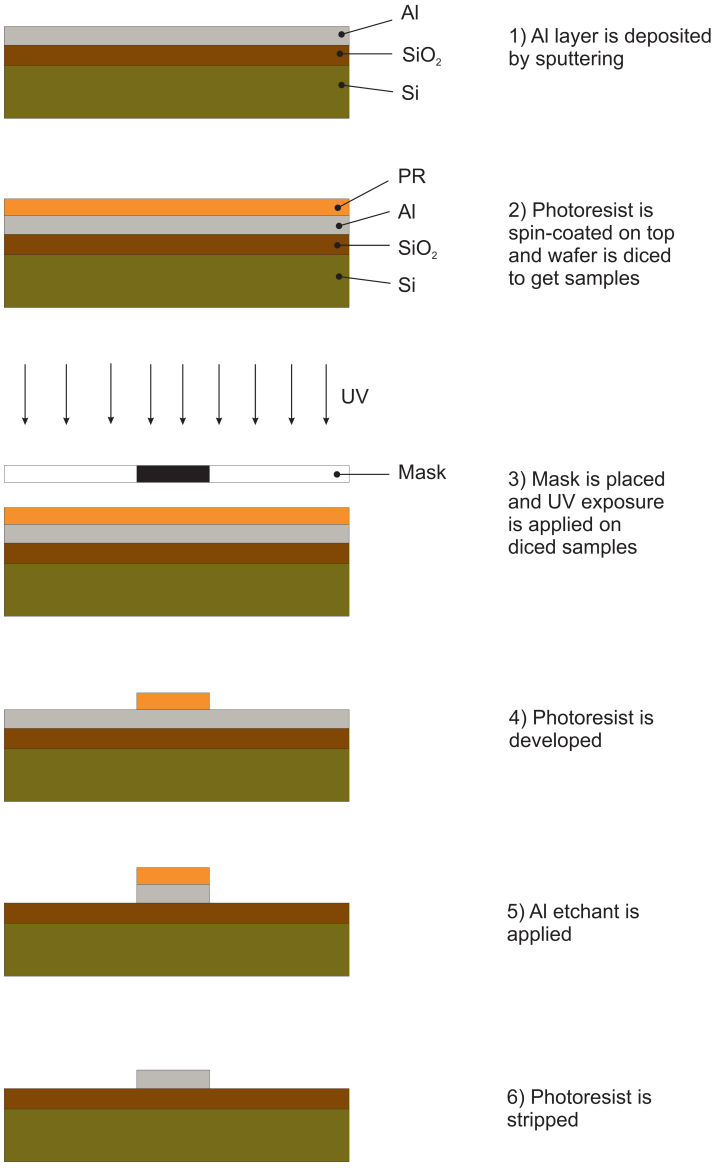

Figure 3.5. Fabrication steps of diode samples.

In Figure 3.5, fabrication steps are shown. Photoresist material is spin-coated onto the Al layer and soft bake at 90° is done for two minutes. Wafer is diced when it is coated with photoresist to minimize the possibility of damaging whole surface and samples are obtained. Then, electrode pattern mask is placed on samples and photoresist is exposed to UV light for 10 minutes. After UV exposure, samples are put in photoresist developer. When photoresist is patterned, Al electrode is formed by using Al etchant. Patterned photoresist protects electrode area being etched. In our

case, photoresist developer can etch the aluminum as well, therefore same material is used as Al etchant. After patterning of Al electrodes is finished, samples are rinsed in acetone, IPA and deionized water respectively as a cleaning procedure. After drying with nitrogen blow, samples are ready for experiments.

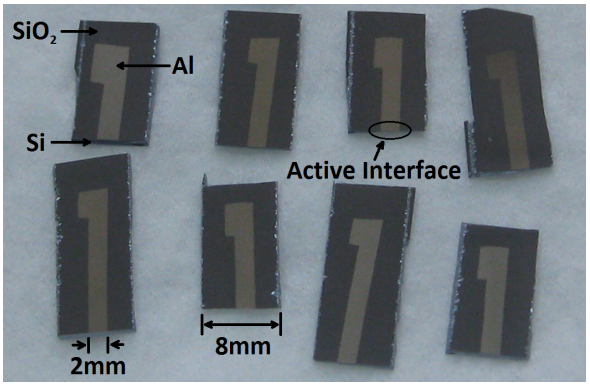

Figure 3.6. Fabricated samples.

In Figure 3.6, obtained samples are shown. Due to the fact that 40 nm oxide is very thin, $Si/SiO_2/Al$ interface at side can easily be contaminated by environment which causes short circuit between two electrodes. To overcome this problem, samples are cleaved just before the lateral diode experiments, therefore polymer solution can be poured onto a clean interface.

To examine the topography, surface and cross-section pictures of samples are taken by scanning electron microscopy (SEM). In Figure 3.7, these pictures are presented.

In Figure 3.7a, the cross-sectional picture can be seen. Due to the fact that oxide part is very thin, it is very hard to distinguish it from the silicon layer. Aluminum and silicon layers are indicated.

In Figure 3.7b, Al layer is exfoliated a little bit at the edge. From this view, the Al thickness can be estimated around 200 nm. Again Si and SiO_2 layers are indistinguishable.

In Figure 3.7c, SiO_2 is slightly etched with buffered HF which does not harm Si part. In the picture two seperate layers can be shown. From this view, approximately 40 nm SiO_2 thickness can be measured which is consistent with the manufacturer's data.

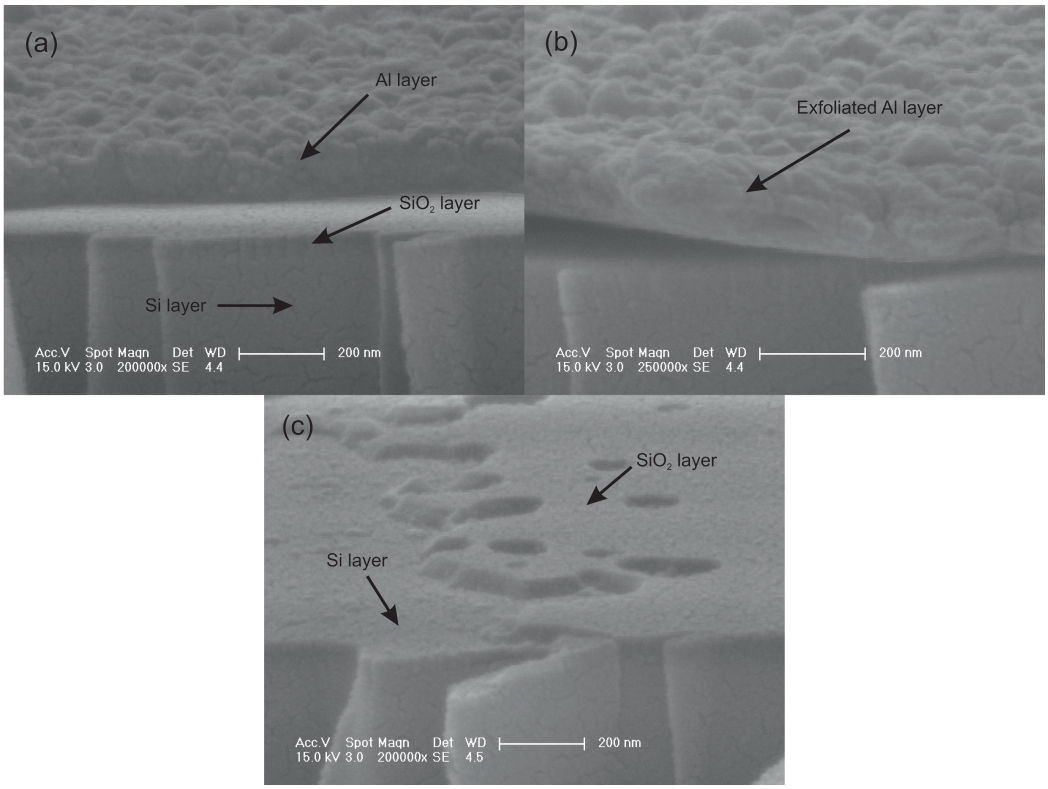

Figure 3.7. SEM pictures of samples. (a) Picture of the interface side. (b) Picture of Al layer. (c) Picture of Si and SiO_2 layers.

With the information about layer thicknesses, final experimental view of the lateral diode is depicted in Figure 3.8. A droplet of polymer solution stays on the $Si/SiO_2/Al$ interface. Estimated arrangement of polymer chains for ideal case is depicted as a magnified view.

3.3. Experimental Work and Characterization

Samples which carry lateral diode structures and polymer semiconductor solutions are prepared for experiments. Some crocodile cables are modified for taking

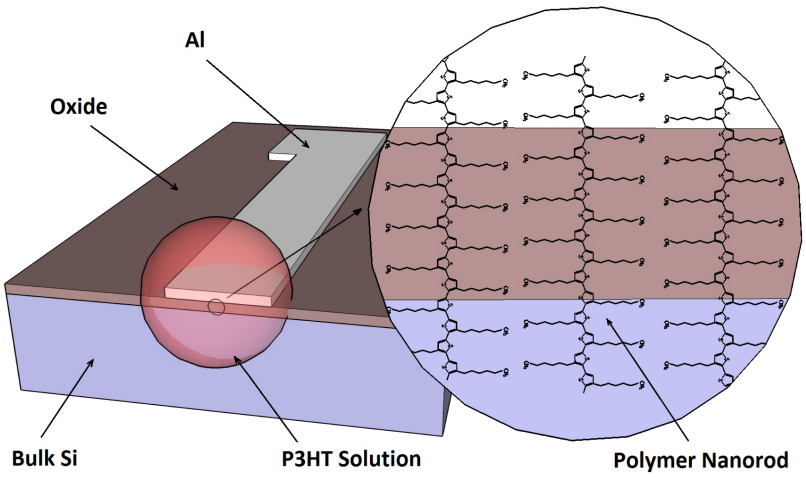

Figure 3.8. Experimental view of lateral diode.

better contacts. Aluminum tips are placed into crocodile cables to prevent Schottky contacts with silicon layer. One important problem was drying of polymer solution which was dripped on the lateral electrode structure. To overcome this situation, a mini pool setup is designed. In this setup, polymer solution is poured into a small container. Instead of dripping solution onto $Si/SiO_2/Al$ interface, sample itself is merged into this container which is filled with polymer solution. Contacts stay out of the solution so contamination of solution due to them is unlikely. Sample is merged suh that the side including interface electrode structure stays at the bottom of the container. If drying occurs, it should start from the polymer solution surface and while drying is progressing electrodes keep staying in the liquid part. Therefore, *liquid state* is preserved for long hours.

In Figure 3.9, experimental setup can be seen. Before measurements are done, solutions are bubbled with nitrogene to get rid of the oxygen dissolved in them. Oxygen introduces ions to the solution and they behave as a parallel resistance to the semiconductor, therefore it is undesirable.

In the measurements, time- and concentration-dependent diode performance characteristics are examined. Also hysteresis effect on diode behavior related to the beginning potential difference is observed. All I-V curve measurements are done with

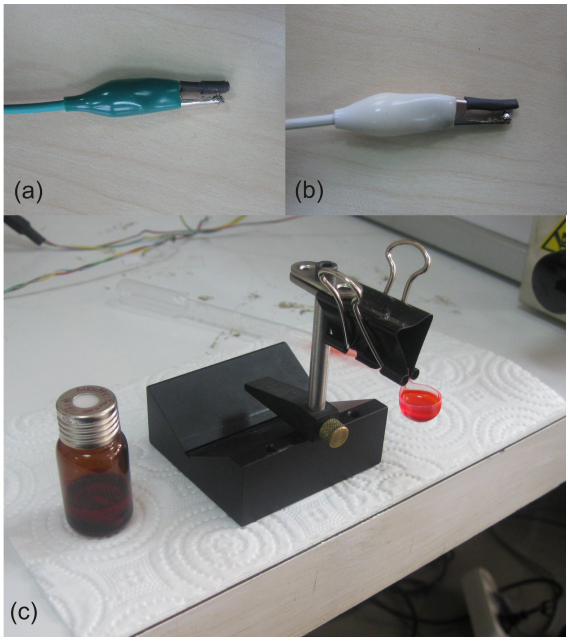

Figure 3.9. Experimental setup is shown. (a) and (b) are modified crocodile cables. (c) is the mini pool setup.

Keithley 4200SCS semiconductor characterization system at room temperature and ambient conditions.

3.3.1. Time-Dependent Performance Measurements

Here, time-dependent performance characteristics of liquid state diodes are measured. Experimental setup is arranged and I-V characteristics are measured with particular time intervals. It is known that oxygen causes degradation [42] and doping [43] on P3HT, therefore we expect a degradation with time in the diode performance.

We obtained the first result with 7.5 mg/ml P3HT:DCB solution. Results are shown in Figure 3.10.

Although degradation with time can be seen, current values may be improved. So, measurements are done with different concentrations. Good observations are achieved with 6 mg/ml P3HT:DCB solution. Results are shown in Figure 3.11 in

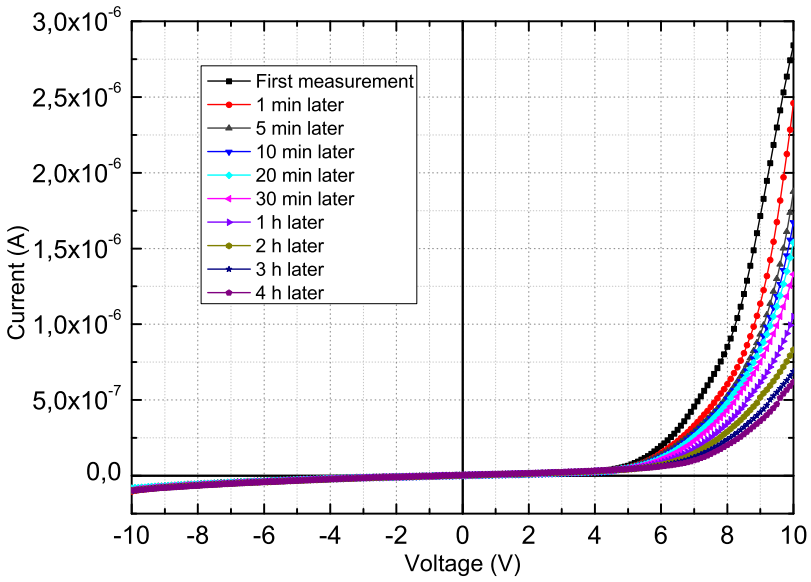

Figure 3.10. Time-dependent diode performance characteristics. Done with 7.5 mg/ml P3HT:DCB solution under ambient conditions. Measurements are taken with indicated time intervals.

semi-log plot. For the sake of clarity, all points are not shown on the graph. Voltage dependence of reverse current indicates the oxygen doping. degradation is more prominent here. After 10 hours, nearly all diode characteristics are diminished. Up to a point, ohmic behavior is seen. Transition from ohmic regime to TCLC regime is not distinct, however it can be identified by examining the slope. Around 4 V, a sudden increase in slope is seen. It is the indicator of transition from TCLC to SCLC regime. It is hard to talk about a square-law relationship at TCLC regime. Therefore it can denote to the existence of deep traps such that an exponential trap distribution on energy levels should be considered instead of discretely distributed shallow traps. Another point is that zero current occurs not at the origin but at -0.7 V. It is the natural result of space-charges and will be revisited in hysteresis measurements.

3.3.2. Concentration-Dependent Performance Measurements

After time-dependent analysis, concentration-dependent measurements are carried. P3HT:DCB solutions are prepared at concentrations of 3 mg/ml, 4.5 mg/ml,

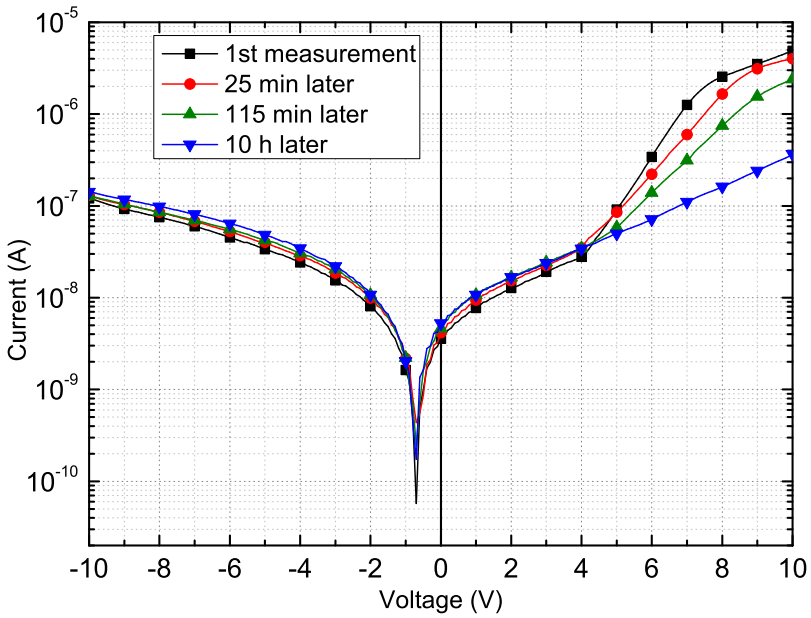

Figure 3.11. Time-dependent diode performance characteristics in semi-log graph. Done with 6 mg/ml P3HT:DCB solution under ambient conditions. Measurements are taken with indicated time intervals.

6 mg/ml, 7.5 mg/ml and 9 mg/ml. Results are shown in Figure 3.12. Due to the fact that differences between curves are not distinct at semi-log graph, results are shown in linear graph. From I-V curves, it can be seen that best performance is obtained with 6 mg/ml solution. Performances of 3 mg/ml and 9 mg/ml are close to each other and they show mediocre performance. The worst performance is shared by 4.5 mg/ml and 7.5 mg/ml.

3.3.3. Hysteresis Effect in Performance Characteristics

All measurements up to now are done by changing applied potential difference from -10 V to $+10$ V. To observe the hysteresis effect, forward and reverse voltage sweeps are done. Semiconductor characterization system is set to high integration time and 100 mV voltage increment/decrement steps. No extra delay time is applied between individual data points. In forward sweep, applied potential difference starts from -10 V and it is increased up to $+10$ V. Reverse sweep, on the other hand, starts with $+10$ V and it is decreased down to -10 V. Forward and reverse sweeps are done

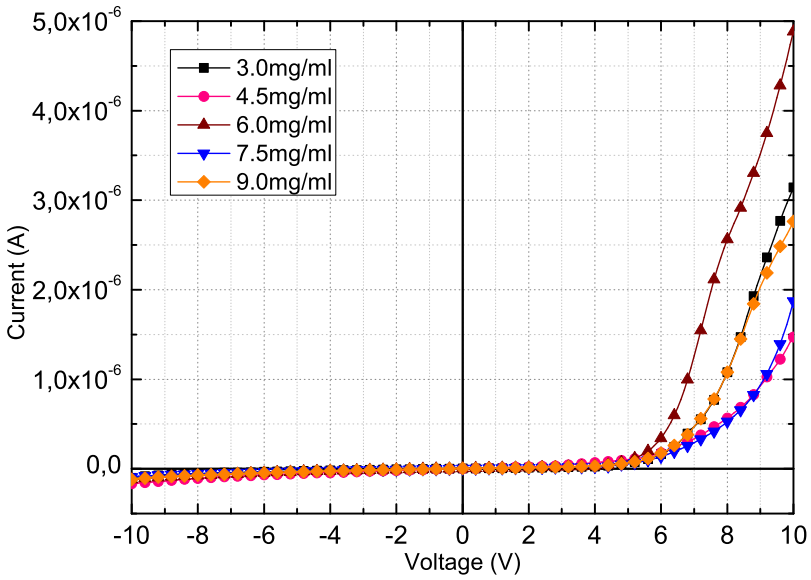

Figure 3.12. Concentration-dependent diode performance characteristics. All measurements are done five minutes after the exposure of solution to ambient atmosphere.

consecutively without any waiting period between them. Measurements are done with 9 mg/ml P3HT:DCB solution and results are shown in Figure 3.13.

For forward sweeps, zero current is observed at -0.7 V. In reverse sweeps, it is around $+1.4$ V. Similar hysteresis results are reported for solid state polymer diodes and OLEDs. This phenomenon is explained with the presence of deep trapped charges in the device. In Chapter 2, charge carrier mobility is assumed to be field-independent in derivations, however it is not always the case. For systems in which charge carrier mobility is field-dependent, mobilities are low at lower biases and traps are not filled [44]. So, after applied potential difference changes, it takes longer to reach the thermal equilibrium. However, it is reported that hysteresis can be prevented by waiting 10 seconds between sweep steps [45].

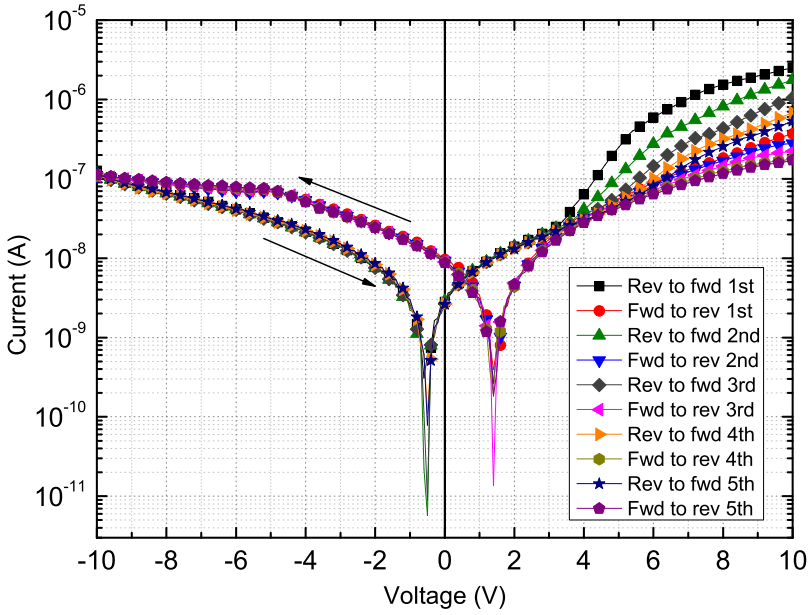

Figure 3.13. Hysteresis effect.

3.3.4. Review and Remarks on Measurements

Liquid state diodes are formed and various measurements are done to analyze their performance characteristics. It is beneficial to take an example I-V curve and re-examine again for review purposes. Here, it is chosen as the first measurement of 6 mg/ml P3HT:DCB solution, because it gave the best performance characteristic during the work. I-V characteristic of the diode with chosen polymer solution can be seen in Figure 3.14. First comment about this plot is the increase of reverse current with increasing voltage. It is an indicator of oxygen doping, therefore there must be trap states. Zero current is observed at -0.7 V which is again related to space-charges and trap states. At two points, slope shows abrupt changes. First one is around 4 V and second is around 7.5 V. However, the graph should be examined in log-log scale to get better opinion about conduction regimes.

In Figure 3.15, this I-V relationship of the liquid state diode is plotted in log-log graph. Slope of the curve between 3 V and 4 V is approximately 1.32, whereas it is 7.81 between 5 V and 7 V and 2.89 between 8 V and 10 V. There is no sharp transition from ohmic region to TCLC region and the slope cannot reach to two before 4 V.

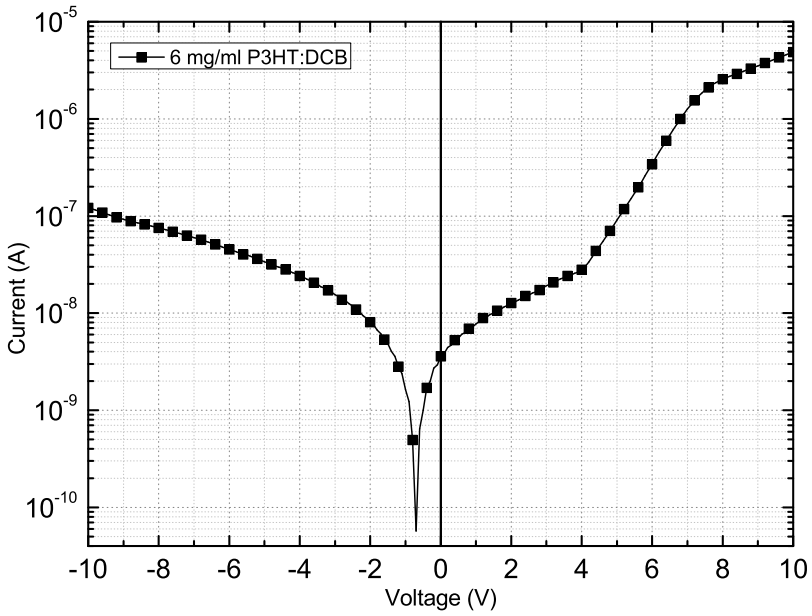

Figure 3.14. I-V curve of the liquid state diode which use 6 mg/ml P3HT:DCB solution. Plotted in semi-log graph.

This behavior can be explained by exponential trap distribution over energy levels. A varying slope value which does not reach to two may indicate that field-independent mobility assumption can be invalid [18]. Between 4 V and 7 V, one can say that trap-filling occurs. After 8 V, slope turns to 2.89. One carrier type SCLC regime shows a quadratic dependence whereas it is cubic for double carrier injection [46]. Therefore, it can be said that after 8 V, conduction does not depend on one type charge carrier anymore.

Including field-dependent mobility, exponential trap distribuiton over energy levels and double carrier injection makes the system so complicated that only numerical solutions can be done.

We can calculate the current density of our system. Current density is determined by the smallest cross-sectional area of layers. It can belong to Al, Si or polymer nano-rod stack. Although it is strongly possible that cross-sectional area of nano-rod stack is smaller than either electrode, there is no way to measure its value. So we can assume that it is equal to cross-sectional area of Al electrode as a worst-case situation. In

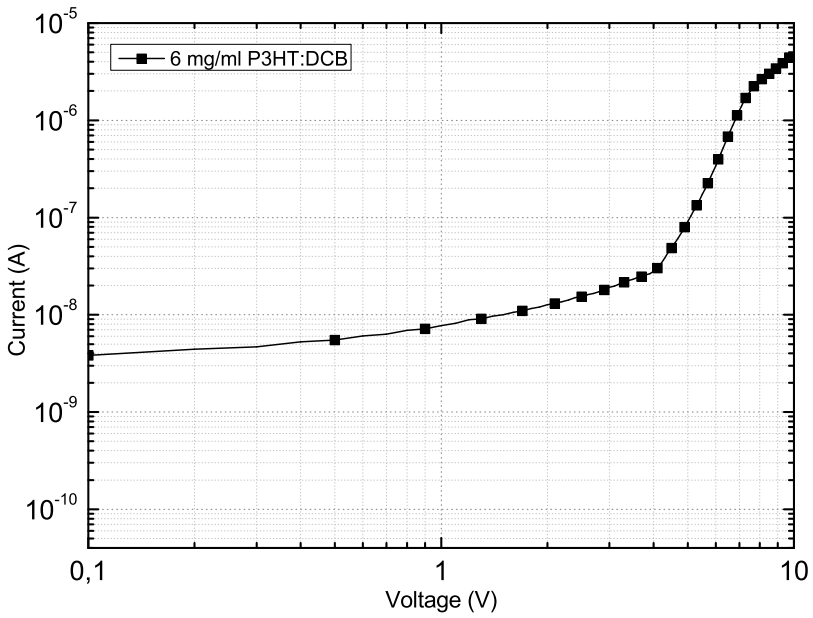

Figure 3.15. I-V curve of the liquid state diode which use 6 mg/ml P3HT:DCB solution. Plotted in log-log graph.

produced samples Al layer has the width of 2 mm and, by SEM measurements, has the approximate thickness of 200 nm. By calculating the area, current density can be found as 315 mA/cm^2 at 7 V. It is not convenient to calculate mobility value from SCLC current density equation by applying I-V measurement data because it can give results orders of magnitude lower than real values [47]. So, it is better to look for other devices at similar voltage values for comparison. Current density is 50 mA/cm^2 for a solid state diode which uses P3HT as semiconductor polymer [48]. Therefore, it can be seen that liquid state diode has at least six fold performance advantage over solid state devices.

4. CONCLUSIONS AND FUTURE WORK

4.1. Conclusions

The main topic of this thesis is the liquid state diode using polymer semiconductor. Its advantages over inorganic counterparts, fabrication process and performance measurements are explained.

In Chapter 1, polymer electronics is introduced. Some application fields and production advantages are mentioned.

In Chapter 2, an overview about physics of polymer semiconductors is done. Atomic background of conduction mechanism and energy bands is explained. Charge carrier injection mechanisms are also mentioned. For conduction process, several regimes and their current-voltage characteristics are analyzed.

In Chapter 3, liquid state diode is explained. Using polymer in solid state bring some disadvantages which are not an issue in liquid phase. Problems about solid state are considered and related solutions which liquid phase usage promises are stated. Possible liquid phase diode structures are examined and their features are discussed. Then, the fabrication of the diode with chosen structure is explained. After realization of the liquid state diode, I-V measurements are done to understand the effects of different variables on diode performance. First, degradation by time is examined. Measurements are done with specific time intervals and I-V curves are obtained. Next, effect of solution concentration is examined. Solutions with different concentrations are prepared and measurements are done. P3HT:DCB solution with concentration of 6 mg/ml is found to be the most efficient one over 3, 4.5, 7.5 and 9 mg/ml solutions. Last measurement was about the hysteresis effect. Back and forth voltage sweeps are applied consecuently to liquid state polymer diode and the hysteresis is observed on obtained I-V curves. At the end of the chapter, an I-V curve is analyzed deeply as a summary and comments are made about the behavior.

4.2. Future Work

Solid state polymer diodes have lots of advantages, yet they have to be optimized and structural problems should be fixed. Microchannel systems suggest good opportunities about liquid state diodes. Polymer solution can be refreshed by proper channels. Disengagement with the atmospheric environment decreases degradation.

Nano-size electrode seperation is an important aspect and should be handled carefully. Energy levels of polymer and electrodes should match for efficient injection and it requires different materials for electrodes. However, it is hard to have nano-size spacing between different materials. If this is achieved properly, performance of liquid state diodes increase and they can be used for application which are otherwise performance-prohibited.

REFERENCES

1. Heeger, A. J., "Nobel Lecture: Semiconducting and Metallic Polymers: The Fourth Generation of Polymeric Materials", *Reviews of Modern Physics*, Vol. 73, No. 3, pp. 681–700, 2001.

2. Voss, D., "Cheap and Cheerful Circuits", *Nature*, Vol. 407, pp. 442–444, 2000.

3. Samuel, I. D. W., "Polymer Electronics", *Philosophical Transactions of the Royal Society of London*, Vol. 358, No. 1765, pp. 193–210, 2000.

4. Forrest, S. R., "The Path to Ubiquitous and Low-Cost Organic Electronic Appliances on Plastic", *Nature*, Vol. 428, pp. 911–918, 2004.

5. Rahman, A., P. Kumar, D. S. Park and Y. B. Shim, "Electrochemical Sensors Based on Organic Conjugated Polymers", *Sensors*, Vol. 8, No. 1, pp. 118–141, 2008.

6. Chaubey, A. and B. D. Malhotra, "Mediated Biosensors", *Biosensors and Bioelectronics*, Vol. 17, pp. 441–456, 2002.

7. Bohm, M., A. Ullmann, D. Zipperer, A. Knobloch, W. H. Glauert and W. Fix, "Printable Electronics for Polymer RFID Applications", *Proceedings of the 2006 IEEE International Solid-State Circuits Conference*, 2006.

8. Bock, K., "Polymer Electronic Systems - Polytronics", *Proceedings of the IEEE*, Vol. 93, No. 8, pp. 1400–1406, 2005.

9. Drury, C. J., C. M. J. Mutsaers, C. M. Hart, M. Matters and D. M. Leeuw, "Low-Cost All-Polymer Integrated Circuits", *Applied Physics Letters*, Vol. 73, No. 1, pp. 108–110, 1998.

10. Gunes, S., H. Neugebauer and N. S. Sariciftci, "Conjugated Polymer-Based Organic Solar Cells", *Chemical Reviews*, Vol. 107, No. 4, pp. 1324–1338, 2007.

11. Tessler, N., *Lectures on Organic Semiconductors and Devices*, 1999, `http://webee.technion.ac.il/people/nir/Lectures.html`, accessed at August 2011.

12. Atkins, P. and J. de Paula, *Physical Chemistry*, 8th edition, W. H. Freeman and Company, New York, 2006.

13. Zumdahl, S. S. and S. A. Zumdahl, *Chemistry*, 8th edition, Brooks Cole, Belmont, 2008.

14. Heeger, A. J., S. Kivelson, J. R. Schrieffer and W. P. Su, "Solitons in Conducting Polymers", *Reviews of Modern Physics*, Vol. 60, No. 3, pp. 781–851, 1988.

15. Coropceanu, V., J. Cornil, D. A. da Silva Filho, Y. Olivier, R. Silbey and J. L. Bredas, "Charge Transport in Organic Semiconductors", *Chemical Reviews*, Vol. 107, No. 4, pp. 926–952, 2007.

16. Klauk, H., *Organic Electronics*, Wiley VCH, Weinheim, 2006.

17. Roichman, Y., *Charge Transport in Conjugated Polymers*, Ph.D. Thesis, Israel Institute of Technology, 2004.

18. Brütting, W., S. Berleb and A. G. Muckl, "Device Physics of Organic Light-Emitting Diodes Based on Molecular Materials", *Organic Electronics*, Vol. 2, No. 1, pp. 1–36, 2001.

19. Campbell, I. H. and D. L. Smith, "Physics of Organic Electronic Devices", *Solid State Physics*, Vol. 55, pp. 1–117, 2001.

20. Melissinos, A. C., *Principles of Modern Technology*, Cambridge University Press, Cambridge, 1990.

21. Sze, S. M., *Physics of Semiconductor Devices*, 2nd edition, John Wiley & Sons, New York, 1991.

22. Mott, N. F. and R. W. Gurney, *Electronic Processes in Ionic Crystals*, Clarendon Press, Oxford, 1940.

23. Montero, J. M., J. Bisquert, G. Garcia-Belmonte, E. M. Barea and H. J. Bolink, "Trap-Limited Mobility in Space-Charge Limited Current in Organic Layers", *Organic Electronics*, Vol. 10, No. 2, pp. 305–312, 2009.

24. Brütting, W., *Lecture Notes: Charge Carrier Injection and Transport in Organic Electronic Devices*, 2007, `http://www.weizmann.ac.il/chemphys/cinaaman/Minerva/Lectures/`, accessed at August 2011.

25. Kao, K. C. and W. Hwang, *Electrical Transport in Solids*, Pergamon Press, Oxford, 1981.

26. Lampert, M. A. and P. Mark, *Current Injection in Solids*, Academic Press, New York, 1970.

27. Takeshita, S., *Modeling of Space-Charge-Limited Current Injection Incorporating an Advanced Model of the Poole-Frenkel Effect*, M.S. Thesis, Clemson University, 2008.

28. McCulloch, I., M. Heeney, C. Bailey, K. Genevicius, I. Macdonald, M. Shkunov, D. Sparrowe, S. Tierney, R. Wagner, W. Zhang, M. L. Chabinyc, R. J. Kline, M. D. McGehee and M. F. Toney, "Liquid-Crystalline Semiconducting Polymers with High Charge-Carrier Mobility", *Nature Materials*, Vol. 5, pp. 328–333, 2006.

29. Heffner, G. W. and D. S. Pearson, "Molecular Characterization of Poly(3-hexylthiophene)", *Macromolecules*, Vol. 24, No. 23, pp. 6295–6299, 1991.

30. Dyreklev, P., M. Berggren, O. Inganas, M. R. Andersson, O. Wennerstrom and T. Hjertberg, "Polarized Electroluminescence from an Oriented Substituted Polythiophene in a Light Emitting Diode", *Advanced Materials*, Vol. 7, No. 1, pp. 43–45, 1995.

31. Perepichka, I. F. and D. F. Perepichka, *Handbook of Thiophene-Based Materials: Applications in Organic Electronics and Photonics*, John Wiley & Sons, West Sussex, 2009.

32. Chan, H. S. O. and S. C. Ng, "Synthesis, Characterization and Applications of Thiophene-Based Functional Polymers", *Progress in Polymer Science*, Vol. 23, No. 7, pp. 1167–1231, 1998.

33. Schopf, G. and G. Koßmehl, "Polythiophenes - Electrically Conductive Polymers", *Advances in Polymer Science*, Vol. 129, pp. 1–166, 1997.

34. Roncali, J., "Conjugated Poly(thiophenes): Synthesis, Functionalization, and Applications", *Chemical Reviews*, Vol. 92, No. 4, pp. 711–738, 1992.

35. Sirringhaus, H., P. J. Brown, R. H. Friend, M. M. Nielsen, K. Bechgaard, B. M. W. Langeveld-Boss, A. J. H. Spiering, R. A. J. Janssen, E. W. Meijer, P. Herwig and D. M. de Leeuw, "Two-Dimensional Charge Transport in Self-Organized, High-Mobility Conjugated Polymers", *Nature*, Vol. 401, pp. 685–688, 1999.

36. Kline, R. J., M. D. McGehee, E. N. Kadnikova, J. Liu and J. M. J. Fréchet, "Controlling the Field-Effect Mobility of Regioregular Polythiophene by Changing the Molecular Weight", *Advanced Materials*, Vol. 15, No. 18, pp. 1519–1522, 2003.

37. Choulis, S., Y. Kim, J. Nelson, D. D. C. Bradley, M. Giles, M. Shkunov and I. McCulloch, "High Ambipolar and Balanced Carrier Mobility in Regioregular Poly(3-hexylthiophene)", *Applied Physics Letters*, Vol. 85, No. 17, pp.

3890–3892, 2004.

38. Li, B. and D. N. Lambeth, "Chemical Sensing Using Nanostructured Polythiophene Transistors", *Nano Letters*, Vol. 8, No. 11, pp. 3563–3567, 2008.

39. Hsu, H. P., W. Paul and K. Binder, "Standard Definitions of Persistence Length Do Not Describe the Local "Intrinsic" Stiffness of Real Polymer Chains", *Macromolecules*, Vol. 43, No. 6, pp. 3094–3102, 2010.

40. Oh, S. W., H. W. Rhee, C. Lee, Y. C. Kim, J. K. Kim and J. W. Yu, "The Photovoltaic Effect of the p-n Heterojunction Organic Photovoltaic Device Using a Nano Template Method", *Current Applied Physics*, Vol. 5, No. 1, pp. 55–58, 2005.

41. Allen, F. G. and G. W. Gobeli, "Work Function, Photoelectric Threshold, and Surface States of Atomically Clean Silicon", *Physical Review*, Vol. 127, No. 1, pp. 150–158, 1962.

42. Schafferhans, J., A. Baumann, C. Deibel and V. Dyakonov, "Trap Distribution and the Impact of Oxygen-Induced Traps on the Charge Transport in poly(3-hexylthiophene)", *Applied Physics Letters*, Vol. 93, No. 093303, pp. 1–3, 2008.

43. Liao, H. H., C. M. Yang, C. C. Liu, S. F. Horng, H. F. Meng and J. T. Shy, "Dynamics and Reversibility of Oxygen Doping and De-Doping for Conjugated Polymer", *Journal of Applied Physics*, Vol. 103, No. 104506, pp. 1–8, 2008.

44. Giulianini, M., E. R. Waclawik, J. M. Bell and N. Motta, "Temperature and Electric Field Dependent Mobility in Poly(3-hexlythiophene)", *Journal of Applied Physics*, Vol. 108, No. 014512, pp. 1–4, 2010.

45. Brütting, W., H. Riel, T. Beierlein and W. Riess, "Influence of Trapped and Interfacial Charges in Organic Multilayer Light-Emitting Devices", *Journal of*

Applied Physics, Vol. 89, No. 3, pp. 1704–1712, 2001.

46. Lampert, M. A., "Double Injection in Insulators", *Physical Review*, Vol. 125, No. 1, pp. 126–141, 1962.

47. Wang, Z. B., M. G. Helander, M. T. Greiner, J. Qui and Z. H. Lu, "Carrier Mobility of Organic Semiconductors Based on Current-Voltage Characteristics", *Journal of Applied Physics*, Vol. 107, No. 034506, pp. 1–4, 2010.

48. Mutlu, S., I. Haydaroglu and A. O. Sevim, "Realization of Charge Pump Circuits Using Polymer Semiconductors", *Organic Electronics*, Vol. 12, No. 2, pp. 312–321, 2011.